Inorg. Chem. **2008**, *47*, 10708−10717

Inorganic Chemistry

Article

Stepwise Modification of Titanium Alkoxy Chloride Compounds by Pyridine Carbinol

Timothy J. Boyle,* Leigh Anna M. Ottley, Mark A. Rodriguez, Robin M. Sewell, Todd M. Alam, and Sarah K. McIntyre

Sandia National Laboratories, Advanced Materials Laboratory, 1001 University Boulevard, SE, Albuquerque, New Mexico 87106

Received February 27, 2008

The stepwise modifications of stoichiometric mixtures of titanium chloride ($TiCl_4$) and titanium *iso*-propoxide ($Ti(OPr^i)_4$) by 2-pyridine methanol (H-OPy) led to the isolation of a systematically varied, novel family of compounds. The 3:1 reaction mixture of $Ti(OPr^i)_4$:$TiCl_4$ yielded $[Cl(OPr^i)_2Ti(\mu\text{-}OPr^i)]_2$ (**1**). Modification of **1** with 1 and 2 equiv of H-OPy produced $[Cl(OPr^i)_2Ti(\mu_c\text{-}OPy)]_2$ (**2**, where μ_c = chelating bridge) and "$(OPy)_2TiCl(OPr^i)$" (**3**, not crystallographically characterized), respectively. Altering the $Ti(OPr^i)_4$ to $TiCl_4$ stoichiometry to 1:1 led to isolation and identification of another dimeric species $[Cl_2(OPr^i)Ti(\mu\text{-}OPr^i)]_2$ (**4**). Upon modification with 1 equiv of H-OPy, $[Cl_2(OPr^i)Ti(\mu_c\text{-}OPy)]_2$ (**5**) was isolated from toluene and $(OPy)TiCl_2(OPr^i)(py)$ (**6**) from py. An additional equivalent of H-OPy led to the monomeric species $(OPy)_2TiCl_2$ (**7**). Because of the low solubility and similarity in constructs of these compounds, additional analytical data, such as the beryllium dome or BeD-XRD powder analyses, were used to verify the bulk samples, which were found to be in agreement with the single crystal structures.

Introduction

To draw meaningful connections between a precursor and the properties of the materials generated from it, the starting compound's structure must be fully understood. For ceramic oxide materials, metal alkoxides ($M(OR)_x$) have come to the forefront as the preferred precursors[1−6] since they are commercially available and the hydrolysis and condensation rates are easily adjusted through the introduction of a wide variety of modifiers. However, the structural aspects of these compounds upon modification can be difficult to predict a priori. A number of issues contribute to their complexity, including the large cation size to small charge ratio that leads to uncontrolled oligomerization through bridging OR ligands, uncontrolled ligand decomposition yielding oxo species, and incomplete ligand exchange. Single crystal X-ray diffraction experiments have proven vital in accurately characterizing these coordination compounds but, unfortunately, growth of X-ray quality crystals is not always possible. Therefore, the controlled construction of $M(OR)_x$ remains an important issue in the development of tailored ceramic materials which is difficult or impossible without structural elucidation of the precursors.

Recently, a series of $(OPy)_2Ti(OR)_2$ (OPy = pyridine carbinoxide) compounds was disseminated where the OR groups were easily substituted through an alcoholysis exchange without altering the central "$(OPy)_2Ti$" core.[7] The constancy of this moiety was attributed to the chelating nature of the OPy ligand imparting chemical stability and preventing structural rearrangement. In an attempt to produce similar stable precursors that were more chemically versatile, the synthesis of $(OPy)_2TiCl_2$ was explored. While developing this route, the stepwise modification of a set of titanium alkoxy chloride (3:1 and 1:1 for $Ti(OPr^i)_4$:$TiCl_4$) species was

---

* To whom correspondence should be addressed. E-mail: tjboyle@Sandia.gov. Phone: (505)272-7625. Fax: (505)272-7336.

(1) Boyle, T. J.; Bunge, S. D.; Andrews, N. L.; Matzen, L. E.; Sieg, K.; Rodriguez, M. A.; Headley, T. J. *Chem. Mater.* **2004**, *16*, 3279.

(2) Boyle, T. J.; Hernandez-Sanchez, B. A.; Baros, C. M.; Brewer, L. N.; Rodriguez, M. A. *Chem. Mater.* **2007**, *19*, 2016.

(3) Hernandez-Sanchez, B. A.; Boyle, T. J.; Baros, C. M.; Brewer, L. N.; Headley, T. J.; Tallant, D. R.; Rodriguez, M. A.; Tuttle, B. A. *Chem. Mater.* **2007**, *19*, 1459.

(4) Boyle, T. J.; Bunge, S. D.; Clem, P. G.; Richardson, J.; Dawley, J. T.; Ottley, L. A. M.; Rodriguez, M. A.; Tuttle, B. A.; Avilucea, G. R.; Tissot, R. G. *Inorg. Chem.* **2005**, *44*, 1588.

(5) Gallegos, J. J.; Ward, T. L.; Boyle, T. J.; Rodriguez, M. A.; Francisco, L. P. *Chem. Vap. Dep.* **2000**, *6*, 21.

(6) Hernandez-Sanchez, B. A.; Boyle, T. J.; Lambert, T. N.; Daniel-Taylor, S. D.; Oliver, J. M.; Wilson, B. S.; Lidke, D. S.; rews, N. L. *IEEE Trans. Nanobiosci.* **2006**, *5*, 222.

(7) Boyle, T. J.; Sewell, R. M.; Ottley, L. A. M.; Pratt, H. D.; Quintana, C. J.; Bunge, S. D. *Inorg. Chem.* **2007**, *46*, 1825.

10.1021/ic801249b CCC: $40.75

elucidated. Equation 1 and Scheme 1 show the stepwise modifications determined in this system as follows: $[Cl(OPr^i)_2Ti(\mu\text{-}OPr^i)]_2$ (**1**), $[Cl(OPr^i)_2Ti(\mu_c\text{-}OPy)]_2$ (**2**), "$(OPy)_2TiCl(OPr^i)$" (**3**), $[Cl_2(OPr^i)Ti(\mu\text{-}OPr^i)]_2$ (**4**), $[Cl_2(OPr^i)Ti(\mu_c\text{-}OPy)]_2$ (**5**), $(OPy)TiCl_2(OPr^i)(py)$ (**6**), and $(OPy)_2TiCl_2$ (**7**) where $OPr^i = OCH(CH_3)_2$, μ_c = chelating bridge, and OPy = $NC_5H_4(CH_2O)$-2. Compounds **1**, **2**, **4**−**7** were crystallographically characterized, with **3** characterized by other analytical means. This report details the synthesis and characterization of the stepwise formation of this family of compounds and describes how the single crystal structures and beryllium dome powder X-ray diffraction (termed BeD-XRD)[8] data were used to characterize the bulk samples of **1**−**7**.

$$x\,Ti(OPr^i)_4 + y\,TiCl_4 + z\,H\text{-}OPy \longrightarrow \text{“}Ti(OPr^i)_a(Cl)_b(OPy)_c\text{”} \tag{1}$$

x	*y*	*z*	"$Ti(OPr^i)_a(Cl)_b(OPy)_c$"	Compound
3	1	0	$[Cl(OPr^i)_2Ti(\mu\text{-}OPr^i)]_2$	**1**
3	1	4	$[Cl(OPr^i)_2Ti(\mu_c\text{-}OPy)]_2$	**2**
3	1	8	'$(OPy)_2TiCl(OPr^i)$'	**3**
1	1	0	$[Cl_2(OPr^i)Ti(\mu\text{-}OPr^i)]_2$	**4**
1	1	2	$[Cl_2(OPr^i)Ti(\mu_c\text{-}OPy)]_2$	**5**
1	1	2	$(OPy)TiCl_2(OPr^i)(py)$	**6**
1	1	4	$(OPy)_2TiCl_2$	**7**

Experimental Section

All compounds described below were handled with rigorous exclusion of air and water using Schlenk line and glovebox techniques. All solvents were stored under argon and used as received (Aldrich) in SureSeal bottles, including hexanes (hex), toluene (tol), and pyridine (py). The following chemicals were used as received (Aldrich and Alfa Aesar): H-OPy, $TiCl_4$, and $Ti(OPr^i)_4$ which was vacuum distilled immediately prior to use.

FT-IR data were obtained on a Bruker Vector 22 Instrument using KBr pellets under an atmosphere of flowing nitrogen. Elemental analyses were performed on a Perkin-Elmer 2400 CHN-S/O Elemental Analyzer. All NMR samples were prepared from dried crystalline materials that were handled and stored under an argon atmosphere. Solid-state ^{13}C cross-polarized magic angle spinning (CPMAS) NMR spectra were obtained on a Bruker Avance 400 at 100.6 MHz using a 4 mm broadband MAS probe. CPMAS NMR spectra were obtained using a standard CP pulse sequence with high power ^1H decoupling, a 1 ms contact time, 20 s recycle delay, 256 scans with a 9 kHz spinning speed. Solution ^1H NMR data were obtained on a 400 MHz Bruker DRX NMR spectrometer with the materials dissolved in the parent deuterated solvent. Yields were not optimized for any of the reactions discussed below.

$[Cl(OPr^i)_2Ti(\mu\text{-}OPr^i)]_2$ (1). $TiCl_4$ (0.129 mL, 1.17 mmol) was added by syringe to a stirring solution of $Ti(OPr^i)_4$ (1.00 g, 3.52 mmol) dissolved in hexanes (∼10 mL) in a 25 mL Schlenk flask, yielding a pale yellow solution. After 30 min, a precipitate formed which easily dissolved upon gentle warming. Upon cooling to room temperature, X-ray quality crystals of **1** were isolated. Crystalline yield 0.983 g (80.6%). FTIR (KBr, cm^{-1}) 2975(s), 2931(m), 2881(m), 2719(w), 2622(w), 1626(w), 1460(m), 1371(s), 1328(m), 1115(s), 1010(s), 927(m), 858(m), 820(m), 619(br, s), 520(sh, m). ^1H NMR (400.1 MHz, tol-d_8) δ 4.75 (1H, sept, $OCH(CH_3)_2$, J_{H-H} = 6.4 Hz) 1.26 (7.8 H, d, $OCH(CH_3)_2$, J_{H-H} = 6.4 Hz). Elem. Anal. Calcd for $C_9H_{21}ClO_3Ti$: C, 41.48; H, 8.12. Found: C, 41.57; H, 8.47.

$[Cl(OPr^i)_2Ti(\mu_c\text{-}OPy)]_2$ (2). To an identical solution described for **1** after warming, H-OPy (0.512 g, 4.69 mmol) was added as quickly as possible by syringe, yielding an insoluble brown precipitate. After stirring for 12 h, the volatile component was removed in vacuo. X-ray quality crystals of **2** were formed by redissolution of the off-white powders in hot toluene and allowing the reaction to cool to glovebox temperature. Crystalline yield 0.568 (39.2%). FTIR (KBr, cm^{-1}) 2971(s), 2926(s), 2869(s), 2693(w), 2616(w), 1605(m), 1468(m), 1441(m), 1366(m), 1323(w), 1285(w), 1262(w), 1169(sh,m) 1128(s), 1043(s), 1021(s), 983(s), 856(m), 820(w), 770(m), 727(w), 646(m), 599(m), 512(s), 472(m,sh). Elem. Anal. Calcd for $C_{12}H_{20}ClNO_3Ti$: C, 46.55; H, 6.510; N, 4.52. Found: C, 46.47; H, 6.62; N, 4.53.

"$(OPy)_2TiCl(OPr^i)$" (3). To an identical solution described for **1** after warming, H-OPy (1.02 g, 9.38 mmol) was added as quickly as possible by syringe, yielding an insoluble brown precipitate. After stirring for 12 h, the volatile component was removed in vacuo. Yield 1.87 g (95.4%). FTIR (KBr, cm^{-1}) 3075(m), 3032(m), 2966(m), 2922(m), 2858(m), 2813(m), 2706(w), 2621(w), 1607(m), 1568(w), 1543(w), 1477(m), 1437(m), 1361(m), 1320(m), 1278(m), 1224(w), 1152(sm), 1126(sh, m), 1095(s), 1047(m), 991(s), 854(m), 823(w), 771(m), 721(m), 649(m), 623(m), 573(m), 522(w), 456(m), 425(w). Elem. Anal. Calcd for $C_{15}H_{19}ClN_2O_3Ti$: C, 50.23; H, 5.34; N, 7.81. Found: C, 50.09; H, 5.79; N, 7.55.

$[Cl_2Ti_2(\mu\text{-}OPr^i)_2]_2$ (4). $TiCl_4$ (0.386 mL, 3.52 mmol) was added by syringe to a stirring solution of $Ti(OPr^i)_4$ (1.00 g, 3.52 mmol) dissolved in hexanes (∼10 mL) in a 25 mL Schlenk flask, yielding a pale yellow solution. After 30 min, a precipitate formed which easily dissolved upon gentle warming. Upon cooling to room temperature, X-ray quality crystals of **4** were isolated. Crystalline Yield 1.02 g (61.5%). FTIR (KBr, cm^{-1}) 2978(s), 2931(m), 1625(m), 1462(m), 1386(m), 1103(s), 1016(s), 938(m), 876(w), 808(m), 631 (brm). ^1H NMR (400.1 MHz, tol-d_8) δ 4.04 (1H, bs, $OCH(CH_3)_2$), 1.10 (7H, bs, $OCH(CH_3)_2$)). Elem. Anal. Calcd. for $C_6H_{14}Cl_2O_2Ti$ (**4**): C, 30.41; H, 5.96. Found: C, 30.54; H, 6.15.

$[Cl_2(OPr^i)Ti(\mu_c\text{-}OPy)]_2$ (5). To an identical solution described for **4** after warming, H-OPy (0.768 g, 7.04 mmol) was added as quickly as possible by syringe, yielding an insoluble brown precipitate. After stirring for 12 h, the volatile component was removed in vacuo. X-ray quality crystals of **5** were formed by redissolution of the off-white powders in hot toluene and allowing the reaction to cool to glovebox temperature. Yield 1.82 g (90.5%). FTIR (KBr, cm^{-1}) 3073(m), 2980(m), 2928(m), 1607(s), 1476(sh,m), 1223(s), 1368(w), 1288(s), 1157(sh, w), 1103(s), 1052(s), 1020(s), 860(m), 820(m), 772(s), 728(s), 648(m), 519(s). ^1H NMR (400.1 MHz, tol-d_8) δ 6.73(1H, dt, $OCH_2(NC_5H_5)$, J_{H-H} = 7.2 Hz), 6.41 (1H, dt, $OCH_2(NC_5H_5)$, J_{H-H} = 8.0 Hz), 6.26 (1H, d, $OCH_2(NC_5H_5)$, J_{H-H} = 8.0 Hz), 5.40 (1H, s(br), $OCH_2(NC_5H_5)$), 5.36 (1H, s(br), $OCH_2(NC_5H_5)$)), 4.76 (1H, s (br), $OCH(CH_3)_2$), 1.26 (6H, d ($OCH(CH_3)_2$). Elem. Anal. Calcd for $C_9H_{13}Cl_2NO_2Ti$: C, 37.80; H, 4.58; N, 4.90. Found: C, 37.30; H, 4.18; N, 4.48.

$(OPy)TiCl_2(OPr^i)(py)$ (6). Compound **2** (1.00 g) was dissolved in py (∼2 mL) and placed in a freezer (−35 °C) until X-ray quality crystals were formed. Crystalline yield 0.704 g (55.2%). FTIR (KBr, cm^{-1}) 3102(m), 3074(m), 2970(s), 2926(m), 2883(m), 2834(m), 1605(s), 1570(w), 1536(m), 1481(s), 1441(s), 1362(m), 1228(m), 1284(m), 1212(m), 1156(m), 1124(s), 1081(s), 1006(s), 859(m), 770(s), 702(m), 651(s), 589(s). ^1H NMR (400.1 MHz, py-d_6) δ 7.70−7.50 (2.1H, mult, $OCH_2(NC_5H_5)$)), 7.25−718 (4.3H, mult, $OCH_2(NC_5H_5)$)), 5.18 (2.8H, s, $OCH_2(NC_5H_5)$)), 3.31 to 5.16(1.1H, mult. $OCH(CH_3)_2$), 1.38 (7.1H, $OCH(CH_3)_2$). Elem. Anal. Calcd for $C_{14}H_{18}Cl_2N_2O_2Ti$: C, 46.06; H, 4.97; N, 7.67. Found: C, 45.67; H, 4.93; N, 7.77.

---

(8) Rodriguez, M. A.; Boyle, T. J.; Yang, P.; Harris, D. L. *Powder Diffr.* **2008**, *23*, 121.

Scheme 1. Chemical Pathway for $Ti(OPr^i)_4$ and $TiCl_4$ Species Modified by HOPy ($OR = OPr^i$)

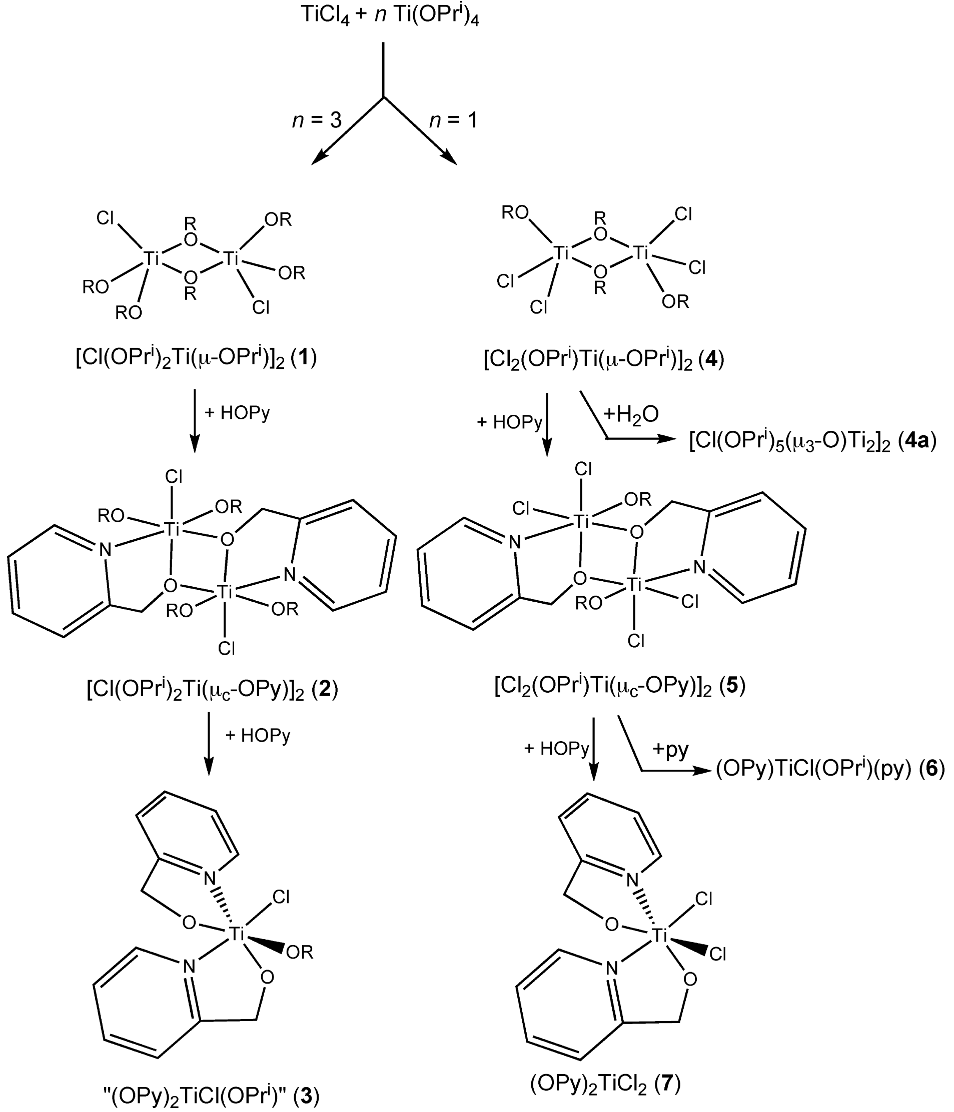

$(OPy)_2TiCl_2$ (7). To an identical solution described for **4** after warming, H-OPy (1.54 g, 14.1 mmol) was added as quickly as possible by syringe, yielding an insoluble brown precipitate. After stirring for 12 h, the volatile component was removed in vacuo. Yield 2.25 g (95.0%). Crystals of **7** were formed by redissolution of the off-white powders in py and allowing the reaction to cool to glovebox temperature. FTIR (KBr, cm^{-1}) 3079(m), 2967(m), 2876(m), 2835(m), 1606(s), 1566(sh, w), 1474(m), 1437(s), 1280(m), 1224(w), 1156(w), 1093(s), 1022(sh, m), 820(w), 773(s), 660(s), 587(m). ^1H NMR (400.1 MHz, py-d_6) δ 8.64 (1H, bs, $OCH_2(NC_5H_5)$), 7.84 (1H, d, $OCH_2(NC_5H_5)$, J_{H-H}= 8.0 Hz), 7.67 (1H, t, $OCH_2(NC_5H_5)$, J_{H-H}= 8.0 Hz), 7.12 (1H, t, $OCH_2(NC_5H_5)$, J_{H-H}= 8.0 Hz), 5.18 (2H, s, $OCH_2(NC_5H_5)$). Elem. Anal. Calcd for $C_{12}H_{12}Cl_2N_2O_2Ti$: C, 43.02; H, 3.61; N, 8.36. Found: C, 43.07; H, 3.76; N, 7.75.

General X-ray Crystal Structure Information.[9,10] Each crystal was mounted onto a thin glass fiber from a pool of Fluorolube and immediately placed under a liquid N_2 stream, on a Bruker AXS diffractometer equipped with an APEX CCD detector. The radiation used was graphite monochromatized Mo Kα radiation ($\lambda = 0.7107$ Å). The lattice parameters were optimized from a least-squares calculation on ~100 reflections. Lattice determination and data collection were carried out using the SMART Version 5.054 software. Data reduction was performed using the SAINT+ Version 6.22 software. The structure refinement was performed using the XSHELL 3.0 software. The data were corrected for absorption using the SADABS (v. 2.05) program within the SAINT software package.

All structures were solved using direct methods, which yielded the heavy atoms, along with a number of the C, H, and O atoms. Subsequent Fourier synthesis generated the remaining atom positions. The final refinement of each compound included anisotropic thermal parameters on all atoms. Structure **2** contains disorder in the terminal *iso*-propoxide ligands that resulted in oblong thermal ellipsoids and a slightly larger refinement value. Additional information concerning the data collection and final structural solutions (Table 1) of these compounds can be found by accessing CIF files through the Cambridge Crystallographic Data Base.

BeD-XRD.[8] BeD-XRD employs a beryllium dome X-ray window (~300 mm thick) that is fastened to a specially designed

---

[9] *Conquest*, Version 1.10; Cambridge Crystallographic Data Centre: Cambridge, U.K.; support@ccdc.cam.ac.uk or www.ccdc.cam.ac.uk [CSD version 5.29 (November 2007].

[10] Allen, F. H. *Acta Crystallogr.* **2002**, *B58*, 380.

Scheme 2. Drawing of the General Aspects of the BeD-XRD Experimental Setup: (A) Assembled and (B) Unassembled with General Dimension 5 × 5 × 2.5 cm

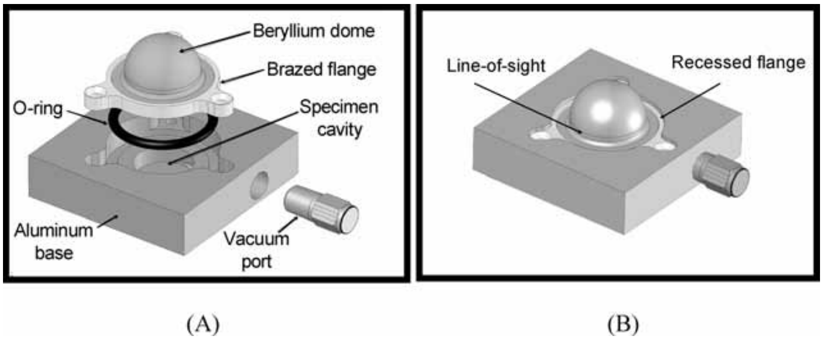

Table 1. Data Collection Parameters for the Crystallographically Characterized Compounds

compound	**1**	**2**	**4**	**4a**
chemical formula	$C_{18}H_{42}Cl_2O_6Ti_2$	$C_{12}H_{20}ClNO_3Ti$	$C_{12}H_{28}Cl_4O_4Ti_2$	$C_{30}H_{70}Cl_2O_{12}Ti_4$
formula weight	521.22	309.64	473.94	885.36
temperature (K)	161(2)	173(2)	173(2)	173(2)
space group	tetragonal, *P*4(3)2(1)2	monoclinic, *P*2(1)/*n*	monoclinic, *P*2(1)/*c*	monoclinic, *P*2(1)/*n*
a (Å)	11.4911(12)	9.1006(10)	8.8120(11)	9.962(2)
b (Å)	11.4911(12)	10.7964(11)	8.1420(10)	18.965(4)
c (Å)	21.426(4)	15.5844(16)	15.2413(18)	12.661(3)
β (deg)		102.346(2)	91.241(2)	102.177(4)
V (Å^3)	2829.2(7)	1495.8(3)	1093.3(2)	2338.1(9)
Z	4	4	2	2
D_{calcd} (Mg/m^3)	1.224	1.375	1.440	1.258
μ(Mo, Kα) (mm^{-1})	0.778	0.750	1.229	0.819
R$_1$^{a} (%) (all data)	4.02 (4.52)	5.05(5.30)	2.11(2.25)	5.24 (6.62)
wR$_2$^{b} (%) (all data)	10.23(10.73)	14.01(14.23)	5.61 (5.77)	12.84 (13.74)

compound	**5**	**6**	**7**
chemical formula	$C_{18}H_{26}Cl_4N_2O_4Ti_2$	$C_{14}H_{18}Cl_2N_2O_2Ti$	$C_{12}H_{12}Cl_2N_2O_2Ti$
formula weight	572.01	365.10	335.04
temperature (K)	173(2)	173(2)	173(2)
space group	monoclinic, *P*2(1)/*n*	monoclinic,	monoclinic, *P*2(1)
a (Å)	8.5829(5)	6.789(7)	8.3354(15)
b (Å)	8.2354(5)	15.487(19)	13.535(2)
c (Å)	17.2773(11)	16.029(16)	12.180(2)
β (deg)	95.0800(10)		90.740(3)
V (Å^3)	1216.43(13)	1685(3)	1374.0(4)
Z	2	4	4
D_{calcd}(Mg/m^3)	1.562	1.439	1.620
μ(Mo, Kα) (mm^{-1})	1.122	0.829	1.009
R$_1$^{a} (%) (all data)	2.97 (3.31)	4.85 (5.06)	5.11 (6.92)
wR$_2$^{b} (%) (all data)	8.21 (8.44)	11.21 (11.30)	8.30 (9.09)

[a] $R1 = \sum||F_o| - |F_c||/\sum|F_o| \times 100$. [b] $wR2 = [\sum w(F_o^2 - F_c^2)^2/\sum(w|F_o|^2)^2]^{1/2} \times 100$.

holder base via set screws, thereby creating a robust seal, via an O-ring separator. A cartoon representation of the BeD-XRD setup is illustrated in Scheme 2.

Since X-ray scatter from the electrons of atoms, X-ray transparency is optimized by the use of low-Z materials. Beryllium is the most reasonable choice for dome fabrication as it is the lightest element that exists as a stable metal under ambient conditions. The dome design essentially eliminates specimen holder artifacts in the 1°−150° 2θ range. However, proper slit configuration is necessary for the exclusion of scatter from the BeD. The O-ring seal is robust whether under an inert gas or vacuum conditions.

All sample preparation was performed in a glovebox where the powder was dispersed on a 1 cm quartz disk (zero-background plate). The powder-coated quartz disk was then pressed into the specimen cavity and leveled to the holder base using a glass slide. The top of the base functions as the defining surface for specimen height, which effectively removes specimen displacement issues. The BeD was placed over the specimen and sealed against the O-ring using three set screws. After assembly, the metal flange of the BeD sits ∼1 mm below the specimen surface and therefore

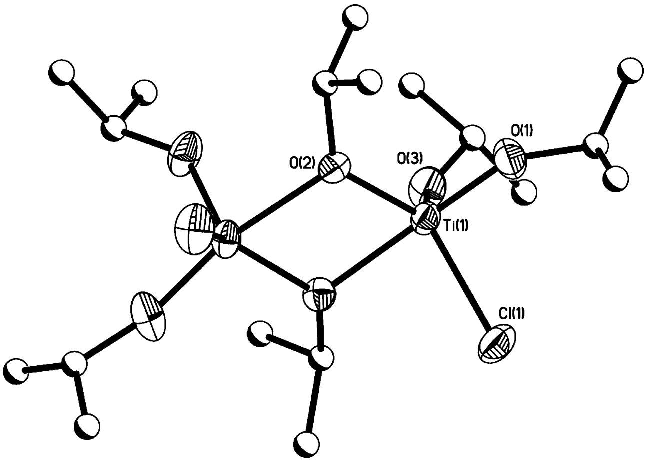

Figure 1. Structure plot of **1**. Heavy atom thermal ellipsoids drawn at 30% level. Carbon atoms drawn as ball and stick and hydrogen atoms omitted for clarity.

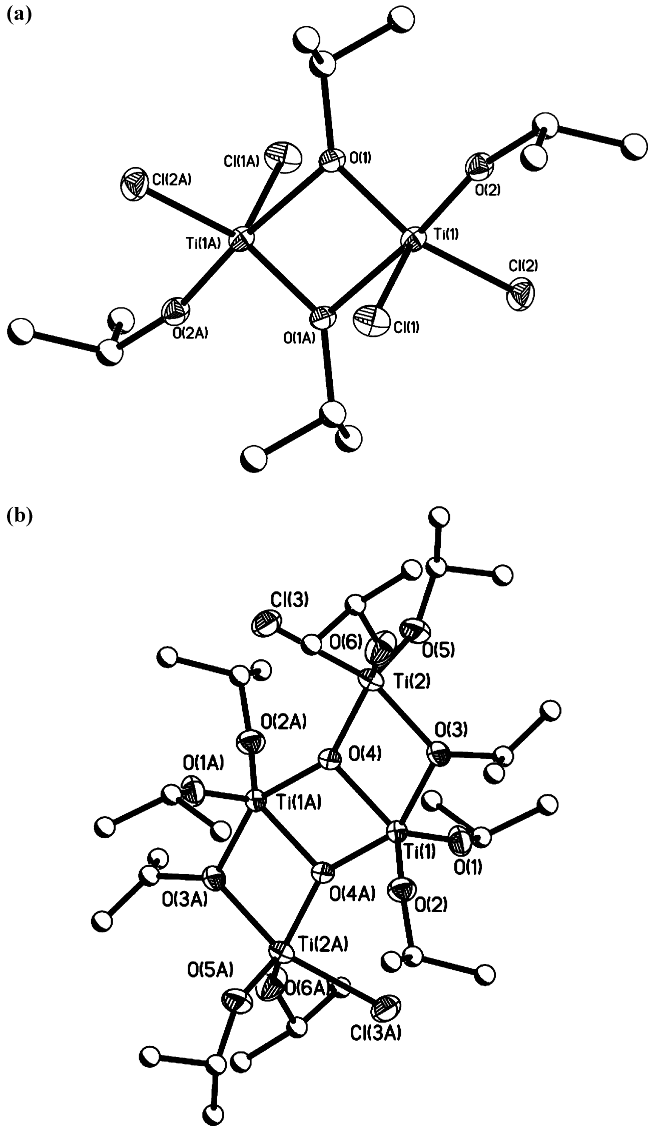

Figure 2. Structure plot of (a) **4** and (b) **4a**. Heavy atom thermal ellipsoids drawn at 30% level. Carbon atoms drawn as ball and stick and hydrogen atoms omitted for clarity.

does not impede the X-ray beam at low diffraction angles. The BeD holder was carefully loaded into a Siemens D500 diffractometer equipped with a sealed-tube Cu X-ray source, a diffracted-beam graphite monochromator, and a scintillation detector. For all scans the instrument settings were 40 kV and 30 mA. Typical scan parameters were 0.04° step-size, a 1 s count-time, and a scan range of 5°−30° 2θ. The diffractometer was run using 1° divergence and receiving slits; the goniometer radius was 250 mm. These conditions assured that the BeD would remain outside the X-ray beam focus and not contribute diffraction signal to the observed powder pattern.

Caution! *Beryllium has been classified as a human carcinogen with symptoms appearing up to decades after the initial contact. The primary health concern is Chronic Beryllium Disease (Beryllicosis) from even minimal exposure to Be-based dusts. Since the BeD-XRD setup employs a solid Be dome, no Beryllicosis hazard is assumed, under standard conditions (a.k.a., SiO$_2$ is not considered a hazard for Silicosis). However, exposure to BeO has also been found to irritate the skin of some people, that can result in a skin disease that makes it difficult for wounds to heal coupled with the possibility of abnormal skin growths (i.e., wart-like bumps). Therefore, it is important that the BeD-XRD setup be handled only by personnel that have had the proper training, wearing the appropriate personal protective equipment (i.e., rubber gloves). If poor handling techniques or any other means shatter the BeD-XRD, proper safety cleanup and disposal protocols* ***must*** *be followed.*

Results and Discussion

Because of the systematic substitution that the (OPy)$_2$Ti(OR)$_2$ system demonstrated without rearrangement,[7] a similar, more chemically versatile compound became of interest. Several metal halide OPy systems had been structurally characterized, including: (O)MCl(OPy)$_2$ (M = Tc,[11] Re[12]),[13] (OPy)AuCl$_2$,[14] (OPy)$_2$RuCl(NO),[15] (OPy)(H-OPy)-RuCl$_2$(NO),[15] Mn$_{12}$(μ_4-O)(μ_3-Cl)$_2$(μ_3-O)$_4$(μ-O$_2$C(C$_6$H$_5$))$_8$-(OPy)$_6$Cl$_2$,[16] Ni$_4$(μ_3-OPy)$_4$(X)$_4$(HOR)$_4$ (X = Cl, Br),[17−20] and Mn$_4$(μ_3-OMe)(OPy)$_4$(μ-NCNCN)$_2$(Br)$_2$;[21] however, no structures were available for Ti with a halide and OPy ligand. Therefore, the initial investigation focused on establishing a set of well-characterized precursors that could be modified with the H-OPy ligand using stoichiometric mixtures of Ti(OPr^i)$_4$ and TiCl$_4$ (eq 1, *xyz* = 310 and 110).

Starting Precursors. In hexanes, upon mixing both the 3:1 and 1:1 reaction mixtures of Ti(OPr^i)$_4$:TiCl$_4$ formed pale yellow solutions. After ~30 min, each reaction formed a precipitate which was easily dissolved upon gentle heating. Upon cooling to room temperature X-ray quality crystals were isolated as **1** (Figure 1) and **4** (Figure 2) for the 3:1 and 1:1 reactions, respectively. Elemental analysis confirmed that the bulk powders were consistent with the single crystal structures. For both compounds, the Ti metal centers were found to adopt a trigonal pyramidal geometry with one OPr^i acting as the bridging species and the respective Cl and OPr^i filling the remaining coordination sites. There was no bound solvent. While a number of TiCl$_x$OR$_{4-x}$ compounds have been structurally characterized, only a hand-full of systems have produced non-solvated species, including [Cl$_2$(OR)Ti(μ-OR)]$_2$ where OR = OEt,[22] OC$_6$H$_5$,[23] OC$_6$H$_4$(Bu^t)-4,[24] and

---

(11) Rochon, F. D.; Melanson, R.; Kong, P.-C. *Inorg. Chim. Acta* **1997**, *254*, 303.

(12) Gerber, T. I. A.; Luzipo, D. G.; Mayer, P. *J. Chem. Crystallogr.* **2005**, *35*, 39.

(13) Boskovic, C.; Brechin, E. K.; Streib, W. E.; Folting, K.; Bollinger, J. C.; Hendrickson, D. N.; Christou, G. *J. Am. Chem. Soc.* **2002**, *124*, 3725.

(14) Hashmi, A. S. K.; Rudolph, M.; Weyrauch, J. P.; Wolfle, M.; Frey, W.; Bats, J. W. *Angew. Chem., Int. Ed.* **2005**, *44*, 2798.

(15) Suzuki, Y.; Tomizawa, H.; Miki, E. *Inorg. Chim. Acta* **1999**, *290*, 36.

(16) Boskovic, C.; Brechin, E. K.; Streib, W. E.; Folting, K.; Hendrickson, D. N.; Christou, G. *Chem. Commun.* **2001**, 467.

(17) Yang, E.-C.; Wernsdorfer, W.; Hill, S.; Edwards, R. S.; Nakano, M.; Maccagnano, S.; Zakharov, L. N.; Rheingold, A. L.; Christou, G.; Hendrickson, D. N. *Polyhedron* **2003**, *22*, 1727.

(18) Yang, E.-C.; Wernsdorfer, W.; Zakharov, L. N.; Karaki, Y.; Yamaguchi, A.; Isidro, R. M.; Lu, G.-D.; Wilson, S. A.; Rheingold, A. L.; Ishimoto, H.; Hendrickson, D. N. *Inorg. Chem.* **2006**, *45*, 529.

(19) Escuer, A.; Font-bardia, M.; Kumar, S. B.; Solans, X.; Vicente, R. *Polyhedron* **1999**, *22*, 1727.

(20) Yang, E.-C.; Kiman, C.; Lawrence, J.; Zakharov, L. N.; Rheingold, A. L.; Hill, S.; Hendrickson, D. N. *Inorg. Chem.* **2005**, *44*, 3827.

(21) Miyasaka, H.; Nakata, K.; Lecren, L.; Coulon, C.; Nakazawa, Y.; Fujisaki, T.; Sugiura, K.; Yamashita, M.; Clerac, R. *J. Am. Chem. Soc.* **2006**, *128*, 3770.

(22) Haase, W.; Hoppe, H. *Acta Crystallogr. Sect. B: Struct. Crystallogr. Cryst. Chem.* **1968**, *24*, 281.

(23) Watenpaugh, K.; Caughlan, C. N. *Inorg. Chem.* **1966**, *5*, 1782.

Table 2. Select Metrical Data for the Crystallographically Characterized Compounds

cmpd	Ti-OPr^{i} (Å)	Ti-(μ-OPr^{i}) (Å)	Ti−O (OPy) (Å)	Ti−O (μ_c-OPy) (Å)	Ti−N (Å)	Ti−Cl (Å)	Ti−Ti(Å)
1	1.76	2.01				2.31	3.21
2	1.78			2.06	2.32	2.36	3.28
4	1.73	2.00				2.26	3.22
4a	1.76	2.01				2.35	3.05
5	1.75			2.00	2.27	2.32	3.22
6	1.73		1.81		2.25	2.36	
7			1.81		2.24	2.35	

cmpd	O−Ti−O	Cl−Ti−Cl	Cl−Ti−O	O−Ti−N	N−Ti−Cl	Ti-(μ_ξ-O)-Ti	(μ-O)-Ti-(μ-O)
1	90.4, 99.2, 101.6, 113.2,167.8		85.7, 91.5, 112.6, 129.5			106.0	73.8
2	88.4, 97.1, 97.8. 102.5. 170.4,		88.9, 97.4, 97.6, 155.3	72.9, 83.8, 89.4, 175.3	86.5	105.7	74.3
4	99.8, 173.9, 74.1	117.6	96.8, 118.9, 86.5, 96.4, 118.2, 86.5			105.9	74.1
4a	93.9, 96.2, 97.6, 97.7, 98.9, 99.0, 112.0, 112.6, 115.0, 122.4, 122.5, 135.4		89.2, 89.9, 97.2, 160.6			102.9, 103.1, 107.2, 149.4	74.8, 77.1, 151.5
5	93.6, 102.5	100.2	89.2, 98.6, 153.9	73.5, 95.0, 169.1	80.5, 88.3	105.6	74.4
6	99.4	92.5	92.9, 94.5, 102.9, 163.6	76.7, 86.2, 90.1, 169.1	87.5, 88.1, 85.0, 166.9		
7	98.8	90.5	94.9, 97.5, 100.8, 161.5	75.4, 76.5, 93.0, 162.1	82.4, 86.5, 96.6, 172.0		

some bidentate ligands (propane-1,3-diolalto[25] and 3,3′-dimethyl-1,1′-bi-2-naphtholato[26]). Some simple HOR solvated compounds have also been isolated such as, $[(HOR)Cl_2(OR)Ti(\mu\text{-}OR)]_2$ where OR = OPr^{i}[27], OCH_2CH_2Cl,[28] $[(HOPr^{i})Cl_2(OPr^{i})Ti(\mu\text{-}Cl)]_2$[27], $[(HOPr^{i})Cl_2(OPr^{i})Ti(\mu\text{-}OPr^{i})]_2$[27], and $[(HOPr^{i})Cl(OPr^{i})_2Ti(\mu\text{-}OPr^{i})]_2$.[29] In general, the metrical data (Table 2) are in agreement for **1** and **4** and with literature[22−29] model compounds. For **1** and **4**, two types (bridging and terminal) of OPr^{i} are expected if the solid state structures were retained in solution; however, the ^{1}H NMR in tol-d_8 of the crystals of **1** and **4** revealed a single set of OPr^{i} resonances. Low temperature ^{1}H NMR investigations did not reveal any additional peaks, merely a loss of resonance intensity for both compounds that was interpreted as crystallization precipitation. This indicates that the dinuclear **1** and **4** are most likely monomeric upon dissolution, which should allow for simple substitutions to occur.

From a reaction mixture of **4** that was set aside for an extended period of time, **4a** (Figure 2b) was isolated. The resultant complex was found to adopt an unusual ladder-like arrangement with μ_3-O, μ-OR, and terminal OR and Cl atoms. The presence of the oxide ligand prevents the third μ-OR typically observed for the M_4O_{12} structure, as noted for $[Cl(OMe)_2Ti(\mu\text{-}OMe)_2(\mu_3\text{-}OMe)Ti(OMe)_2]_2$.[30] The Cl atoms in **4a** are preferentially metathesized presumably from adventitious water yielding an oxo species. Further determination of a rational pathway to this compound is underway but, because of the unusual ladder-like central core, the structure is reported here.

Monosubstitution by HOPy. With the identity of **1** and **4** established, structural modifications by HOPy were undertaken (see Scheme 1). The addition of 1 equiv of HOPy to 3:1 and 1:1 $Ti(OPr^{i})_4/TiCl_4$ reaction mixtures led immediately to brown precipitates that under vaccuum-dried to pale white powders. The FTIR data indicated that both bulk powders possessed an OPy ligand along with Ti−O stretches. Single crystal X-ray diffraction results of crystals isolated from toluene revealed that the OPy ligand had successfully modified both **1** and **4**, yielding **2** (Figure 3a) and **5** (Figure 4), respectively. These compounds adopt similar dinuclear arrangements with the O atom of the OPy ligand forming a bridge and the N of the ring binding to the octahedrally (Oh) coordinated Ti metal centers. In the literature there are only seven Ti compounds[31−36] with one Cl, one N, and four O atoms completing an Oh geometry with none represented by the combination of OR, Cl, and OPy ligands found in **2**. Metrical data for **2** compares favorably with these compounds and those noted for **1** (Table 2). Elemental analyses of the bulk powders were in agreement with the single crystal structure.

Solid-state ^{13}C CPMAS NMR spectra (Figure 5) were collected on the bulk powders of **2** (Figure 5a) and **5** (Figure 5c). The appropriate ^{13}C shifts for the carbons of the two

---

(24) Nielson, A. J.; Shen, C.; Schwerdtfeger, P.; Waters, J. M. *Eur. J. Inorg. Chem.* **2005**, *7*, 1343.

(25) Huang, Y.; Stephan, D. W. *Can. J. Chem.* **1995**, *73*, 956.

(26) Boyle, T. J.; Eilerts, N. W.; Heppert, J. A.; Takusagawa, F. *Organometallics* **1994**, *13*, 2218.

(27) Wu, Y.-T.; Ho, Y.-C.; Lin, C.-C.; Gau, H.-M. *Inorg. Chem.* **1996**, *35*, 5948.

(28) Winter, C. H.; Sheriden, P. H.; Heeg, M. J. *Inorg. Chem.* **1991**, *30*, 1962.

(29) Nunes, G. G.; Reis, D. M.; Camargo, P. H. C.; Hitchcock, P. B.; Homer, M.; Matos, R. M.; Mangrich, A. S.; Sa, E. L. D.; Leigh, G. J.; Soares, J. F. *J. Braz. Chem. Soc.* **2003**, *14*, 922.

(30) Hyvarinen, K.; Kinga, M.; Leskela, M. *Acta Chem. Scand.* **1995**, *49*, 820.

(31) Doherty, S.; Errington, R. J.; Housley, N.; Ridland, J.; Clegg, W.; Elsegood, M. R. J. *Organometallics* **1999**, *18*, 1018.

(32) Muller, J.; Kehr, G.; Frohlich, R.; Erker, G. *Eur. J. Inorg. Chem.* **2005**, *14*, 2836.

(33) Owiny, D.; Parkin, S.; Ladipo, F. T. *J. Organomet. Chem.* **2003**, *678*, 134.

(34) Suzuki, Y.; Oshiki, T.; Tanaka, H.; Takai, K.; Fujita, T. *Chem. Lett.* **2005**, *34*, 1458.

(35) Hintermann, L.; Broggini, D.; Togni, A. *Helv. Chim. Acta* **2002**, *85*, 1597.

(36) Chan, M. C. W.; Tam, K.-H.; Pui, Y.-L.; Zhu, N. *J. Chem. Soc., Dalton Trans.* **2002**, 3085.

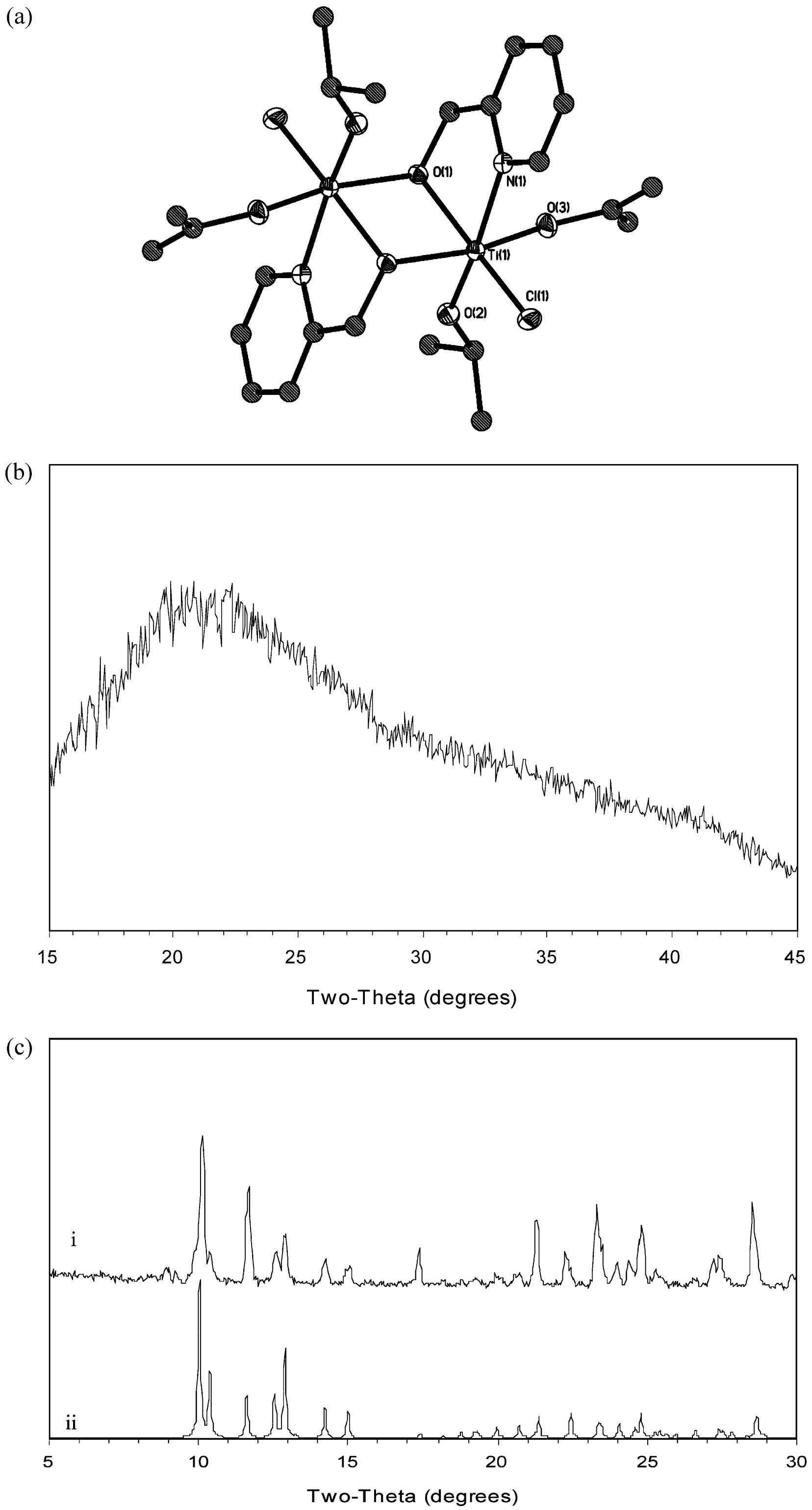

Figure 3. (a) Structure plot of **2**. Heavy atom thermal ellipsoids drawn at 30% level. Carbon atoms drawn as ball and stick and hydrogen atoms omitted for clarity. (b) micro-XRD of **2**, and (c) BeD-XRD of **2**: (i) experimental versus (ii) calculated XRD pattern.

types of OPr^i (bridging and terminal) and single OPy were observed for both samples. BeD-XRD was employed to assist in the further characterization of air-sensitive bulk powders.[8] Comparison of the experimental powder pattern via BeD-XRD to that of the calculated powder XRD pattern derived from the single crystal structure enables a straightforward method for phase confirmation of bulk powders. This method has been found to be an improvement in comparison to microXRD or bag encapsulation methods because of the higher signal to noise ratio achieved. For example, the pattern obtained by microXRD on compound **2** assisted little in terms of the bulk characterization (Figure 3b). In contrast, the BeD-XRD pattern of **2** displays a great deal more information (Figure 3c-i) and was favorably compared to its calculated pattern (Figure 3c-ii). The general appearance of peak positions and approximate peak heights were evaluated for

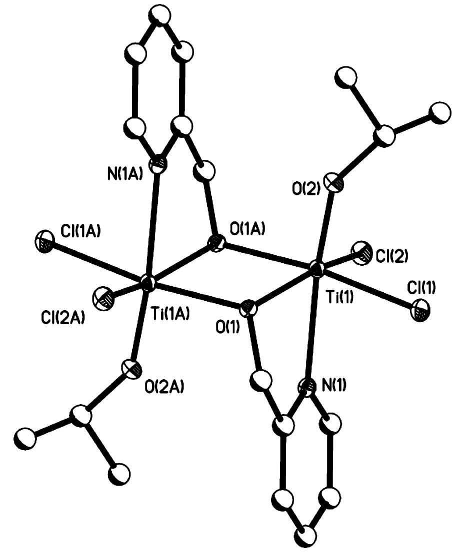

Figure 4. Structure plot of **5**. Heavy atom thermal ellipsoids drawn at 30% level. Carbon atoms drawn as ball and stick and hydrogen atoms omitted for clarity.

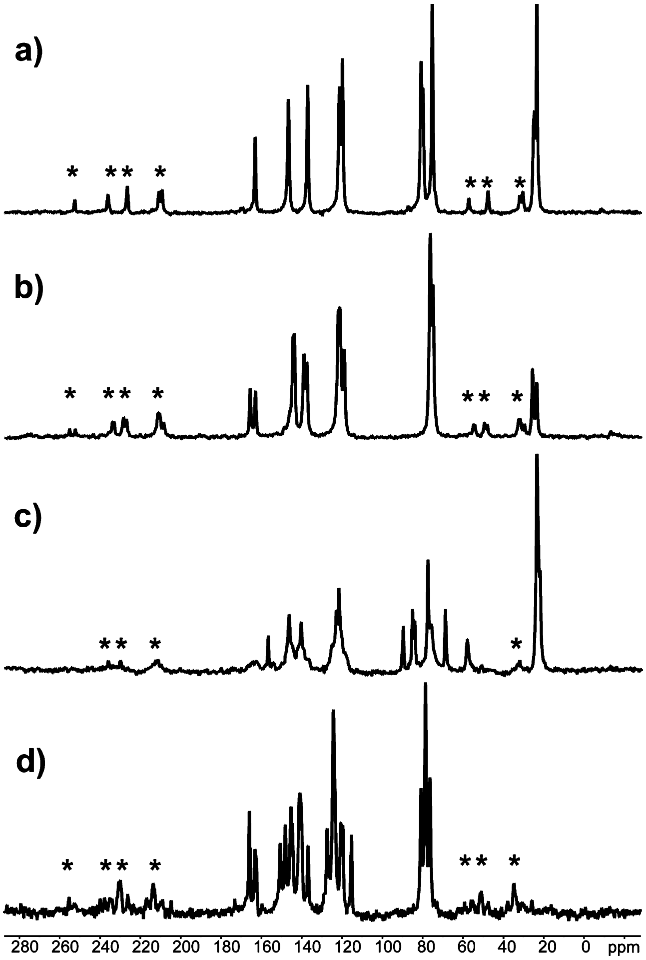

Figure 5. Solid-state ^{13}C CPMAS NMR of (a) **2**, (b) **3**, (c) **5**, (d) **7**. Spinning sidebands are denoted by *.

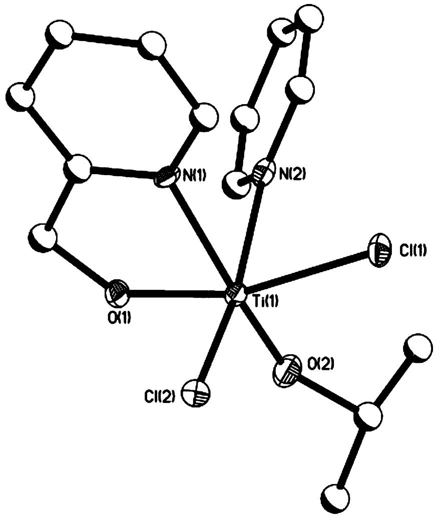

Figure 6. Structure plot of **6**. Heavy atom thermal ellipsoids drawn at 30% level. Carbon atoms drawn as ball and stick and hydrogen atoms omitted for clarity.

the observed (3c-i) and calculated patterns (3c-ii). As is typical for nonidealized powder XRD patterns, there is some expected variability of peak intensities because of preferential orientation of crystalline morphologies when analyzed in powdered form. In particular, the (022) peak at ~17.1° 2θ showed exaggerated peak intensity in the experimental pattern (Figure 3c-i) as compared to its calculated pattern. After evaluating the (022) plane and its relative orientation to the packing arrangement of **2** in the host lattice, the "extra" observed peak is believed to be due to preferred crystal orientation effects. In general, however, the BeD-XRD patterns supported the identification of the bulk powder as consistent with the crystal structure obtained.

Because of the relative insolubility of **2** in tol-d_8 at room temperature, meaningful solution state NMR data could not be obtained. The solubility of **5** in tol-d_8 was very low as well, but limited information was garnered. The ^{1}H NMR spectrum of the free H-OPy in tol-d_8 displays a methylene resonance at 4.53 ppm, whereas for **5**, two methylene resonances were observed at 5.40 and 5.36 ppm in a 1:1 ratio. Variable temperature (-20 to $+60$ °C) solution ^{1}H NMR spectra were obtained, and the OPy ligand resonances were found to shift in a manner consistent with the (OPy)$_2$Ti(OR)$_2$ system,[7] wherein, the OPy most likely oscillates between chelating and monodentate binding modes.

Introduction of a small amount of py to a toluene solution of **5** led to rapid dissolution of the insoluble material. From a concentrated solution at room temperature, X-ray quality crystals were easily isolated and solved as **6** (see Figure 6). The Ti metal center of compound **6** was found to be an Oh bound monomer with two terminal chlorides, a terminal OPr^i, a chelating OPy ligand, and the first example of py coordinating to the metal center of an OPy ligated species. There is a structurally characterized (Cp)Ti(OPy)(OPr^i)$_2$ complex that resembles **6**; however, it uses the much more sterically hindering Cp ligand to maintain these characteristics.[37] IR data and elemental analyses of the bulk powder are consistent with the crystal structure. Solution ^{1}H NMR of H-OPy in py-d_5 has a methylene resonance at 5.15 ppm. For **6**, the shift to 5.76 ppm, indicated the presence of a bound OPy; however, while the peak is broad but at room

---

(37) Doherty, S.; Errington, R. J.; Jarvis, A. P.; Collins, S.; Clegg, W.; Elsegood, M. R. J. *Organometallics* **1998**, *17*, 3408.

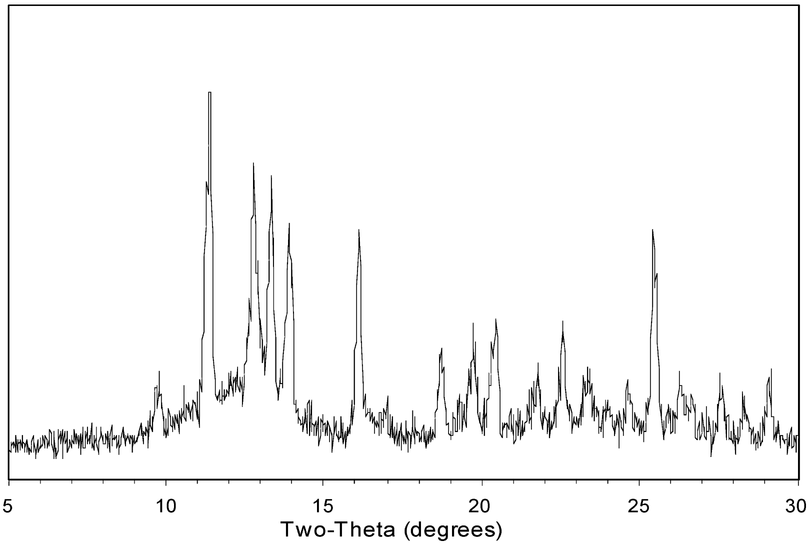

Figure 7. BeD-XRD of bulk powder of **3**.

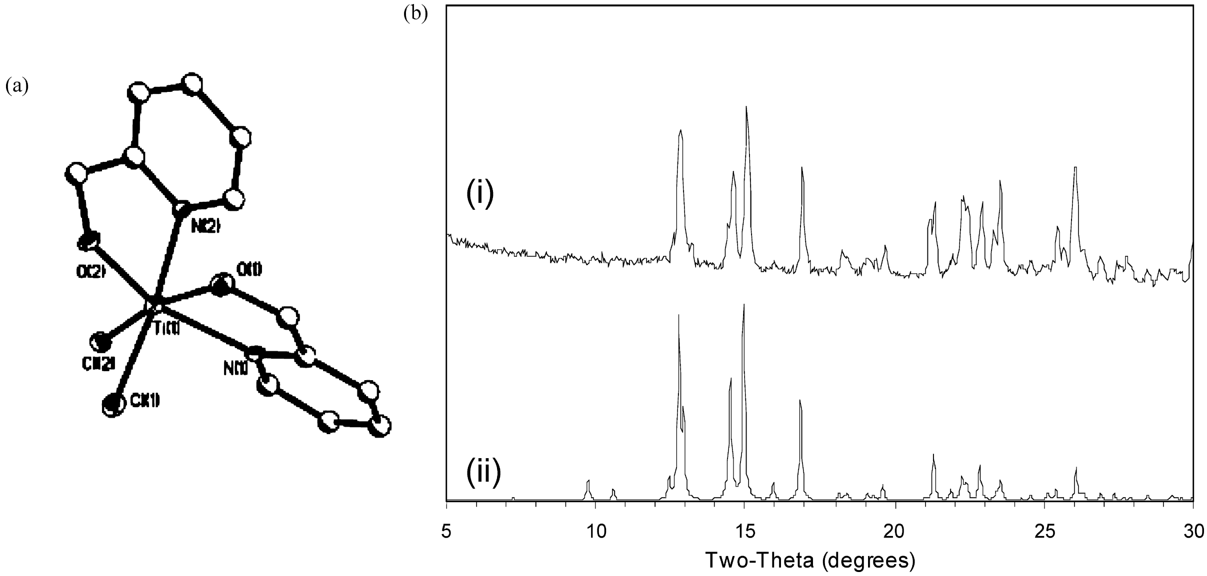

Figure 8. (a) Structure plot of **7**. Heavy atom thermal ellipsoids drawn at 30% level. Carbon atoms drawn as ball and stick and hydrogen atoms omitted for clarity. (b) BeD-XRD of **7**: (i) experimental versus (ii) calculated XRD pattern.

temperature, two peaks were *not* observed. Further, the OPr^i resonances were present in the appropriate ratio. Therefore in the parent solvent, the structure appears to be retained. With this success in isolation of **6**, compound **2** was redissolved in py, stirred overnight, and crystallized. In contrast to **6**, this recrystallization of **2** in py yielded no coordinated py.

Disubstitution by H-OPy. Synthesis of the disubstituted complexes were undertaken through the addition of two equivalents of H-OPy to 3:1 or 1:1 reaction mixtures to generate **3** or **7**, respectively. Upon addition of the H-OPy (eq 1), an oily brown precipitate formed immediately which led to tan powders when dried. These powders proved to be insoluble in hot toluene but readily dissolved in py. X-ray quality crystals of **3** were never isolated but the analytical data collected did give some insight into the potential structure, preliminarily assigned as "$(OPy)_2TiCl(OPr^i)$" (**3** shown in Scheme 1). FTIR data indicated the presence of both the OPy and OPr^i ligands; the ^{13}C CPMAS NMR data (Figure 5b) revealed the presence of two inequivalent OPy ligands; elemental analysis was consistent with the empirical formula; solution NMR did not yield useful information because of the low solubility of **3**. The overall monomeric nature and asymmetric substitution was deduced based on the numerous previous disubstituted monomeric species isolated for the $(OPy)_2Ti(OR)_2$ series and $(OPy)_2Ti(OPr^i)$-$(OC(Me)CH_2Me)$.[7] A possible unit cell for the BeD-XRD observed pattern (Figure 7) was determined as: monoclinic $a = 12.60(1)$ Å, $b = 10.31(2)$ Å, $c = 19.89(2)$ Å, $\beta = 106.2(1)°$, $V = 2478(3)°$ Å^3.

Compound **7** was found to be highly soluble in py and easily formed crystals; however, the material rapidly reacted with the oil (Fluorolube) used to cover the crystals or when mounted on the goniometer were of poor quality. Fortunately, one crystal was isolated, mounted, and solved as **7** (shown in Figure 8a). The geometry of the Ti metal centers was found to be Oh with two chelating OPy ligands and two terminal Cl ligands. The general structural aspects of 7 are similar to that of the previously reported $(OPy)_2Ti(OR)_2$ species[7] and somewhat reminiscent of the widely used $(Cp)_2TiCl_2$[38−43] system. The metrical data is fully consistent with the literature $(OPy)_2Ti$ compounds[7] and the structures noted here (Table 2). The elemental analysis of the bulk powder was found to be consistent with the crystal structure. Solid state ^{13}C CPMAS NMR data indicates the presence of only OPy ligands (Figure 5d) and solution ^1H NMR data revealed only the presence of the OPy ligand at δ 5.17 with no resonances associated with OPr^i ligands. Because of the difficulty in obtaining crystals, a BeD-XRD study was undertaken to aid in identification of the bulk powder. A comparison of the peak positions and intensities of the experimental versus the calculated pattern (Figure 8b-i) indicated that the bulk powder was consistent with the single crystal structure pattern.

Summary and Conclusion

The systematic alcoholysis of the fully characterized $Ti(OPr^i)_4/TiCl_4$ (3:1, 1:1) by stoichiomeric additions of H-OPy has been structurally characterized (eq 1) yielding the mono and disubstituted species (see Scheme 1, eq 1). Because of the limited solubility and difficulty in crystallizing some of these compounds, the bulk powders of these compounds were additionally characterized using BeD-XRD. This method has proven extremely useful in elucidating the identity of the bulk, air-sensitive powders. The unusual controlled modification noted for this system allows for systematic variations of the precursors for tailored applications with specificity not achievable in other systems. Because of this tunability, the catalytic behavior of these compounds as they pertain to the polymerization of olefins is underway. Additionally, the structural similarity and increased stability of **7** in comparison to the anticancer agent $(Cp)_2TiCl_2$,[44−47] has led to cancer cellular studies of **7** as a novel therapeutic agent.

Acknowledgment. The authors thank Dr. C. Stewart (SNL) for helpful discussions and for support of this research, the Office of Basic Energy Science of the U.S. Department of Energy under Contract DE-AC04-94AL85000. Sandia is a multiprogram laboratory operated by Sandia Corporation, a Lockheed Martin Company, for the United States Department of Energy.

Supporting Information Available: Compound structures in CIF format. This material is available free of charge via the Internet at http://pubs.acs.org. The crystal structures for **1**−**7** have been deposited at the Cambridge Crystallographic Data Centre and allocated the deposition numbers CCDC 692062−692068.

IC801249B

---

(38) Endo, K.; Nomaguchi, T.; Tsuchiya, Y. *J. Polym. Sci., Part A: Polym. Chem.* **2007**, *45*, 3872.

(39) Ponce-Ibarra, V. H.; Benavides, R.; Cadenas-Pilego, G.; Maldonado, H. *Polym. Degrad. Stab.* **2007**, *92*, 249.

(40) Noh, S. K.; Jung, W. S.; Oh, H.; Lee, Y. R.; Lyoo, W. S. *J. Organomet. Chem.* **2006**, *691*, 5000.

(41) Magdesieva, T. V.; Graczyk, M.; Vallat, A.; Nikitin, O. M.; Demyanov, P. I.; Butin, K. P.; Vorotyntsev, M. A. *Electrochim. Acta* **2006**, *52*, 1265.

(42) Ponce-Ibarra, V. H.; Benavides, R.; Cadenas-Pilego, G.; Palos-Pizarro, I.; Huerta, B. M. *Polym. Degrad. Stab.* **2006**, *91*, 499.

(43) Asandei, A. D.; Moran, I. W.; Saha, G.; Chen, Y. H. *J. Polym. Sci., Part A: Polym. Chem.* **2006**, *44*, 2015.

(44) Kratz, F.; Schutte, M. T. *Cancer J.* **1998**, *11*, 60.

(45) Caruso, F.; Rossi, M.; Pettinari, C. *Expert Opin. Ther. Pat.* **2001**, *11*, 969.

(46) Caruso, F.; Rossi, M. *Mini-Rev. Med. Chem.* **2004**, *4*, 49.

(47) Harding, M. M.; Mokdsi, G. *Curr. Med. Chem.* **2000**, *7*, 1289.